

CAUSAL ANALYSIS OF INNER AND OUTER MOTIONS IN NEAR-WALL TURBULENT FLOW

Jingxuan Zhang

Center for Particle-Laden Turbulence
Lanzhou University
Lanzhou, China

Zhengping Zhu

Zhejiang Laboratory
Hangzhou, China

Ricardo Vinuesa

FLOW, Engineering Mechanics
KTH Royal Institute of Technology
Stockholm, Sweden
Email: rvinuesa@mech.kth.se

Ruifeng Hu

Center for Particle-Laden Turbulence
Lanzhou University
Lanzhou, China
Email: hurf@lzu.edu.cn

ABSTRACT

In this work, we study the causality of near-wall inner and outer turbulent motions. Here we define the inner motions as the self-sustained near-wall cycle and the outer motions as those living in the logarithmic layer exhibiting a footprint on the near-wall region. We perform causal analysis using two different methods: one is the transfer entropy, based on the information theory, and the other one is the Liang–Kleeman information-flow theory. The causal-analysis methods are applied to several scenarios, including a linear and a non-linear problem, a low-dimensional model of the near-wall cycle of turbulence, as well as the interaction between inner and outer turbulent motions in a channel at a friction Reynolds number of $Re_\tau = 1000$. We find that both methods can well predict the causal links in the linear problem, and the information flow can identify more of the nonlinear problem. Despite richer causalities revealed by the transfer entropy for turbulent-flow problems, both methods can successfully identify the streak-vortex regeneration mechanism that majorly sustains the near-wall turbulence. It is also indicated that both bottom-up and top-down influences of inner and outer motions may coexist in addition to the multiscale self-sustaining mechanism. Lastly, we mention that the computation of the information flow is much more efficient than the transfer entropy. The present study suggests that the information flow can have great potential in causal inference for turbulent-flow problems besides the transfer entropy.

INTRODUCTION

It is well known that wall-bounded turbulent flows are populated with energy-containing coherent structures spanning a wide range of spatial and temporal scales (Robinson, 1991; Adrian, 2007; Smits *et al.*, 2011; Jiménez, 2018), *e.g.* streamwise streaks, hairpin vortices, large-scale motions, very-large-scale motions and superstructures among others. An open question is what are the causal links of these turbulent motions, especially in the context of inner and outer motions, either bottom-up (Adrian *et al.*, 2000), top-down (Hunt & Morrison, 2000), co-supporting (Toh & Itano, 2005;

Zhou *et al.*, 2022) or independently self-sustained at all scales (Cossu & Hwang, 2017). For this purpose, We resort to the two widely adopted metrics which have been applied in physics, atmospheric sciences as well as fluid dynamics research recently, *i.e.* the transfer entropy (Schreiber, 2000) and the Liang–Kleeman information flow (Liang & Kleeman, 2005; Liang, 2013, 2014, 2016). Here we define the inner motions as the universal near-wall cycle (Hamilton *et al.*, 1995; Waleffe, 1997), and the outer motions as those living in the logarithmic layer exhibiting a footprint on the near-wall region (Hutchins & Marusic, 2007; Marusic *et al.*, 2010).

METHODOLOGY

Inner-outer decomposition of near-wall turbulent motions

The turbulent-flow velocity components of inner and outer motions are decomposed by a scaling-improved inner-outer decomposition method (Wang *et al.*, 2021a), which is generally based on the predictive inner-outer model (PIOM) (Marusic *et al.*, 2010; Mathis *et al.*, 2011; Baars *et al.*, 2016). In the PIOM, the near-wall turbulent-flow velocities can be decomposed by $u_i = u_{i,S} + u_{i,L}$, where u_i is the turbulent-flow velocity in the i th direction, $u_{i,S}$ is the small-scale velocity of the inner motions or near-wall cycle modulated by large-scale outer footprint velocity $u_{i,L}$.

The large-scale outer footprint velocity is calculated by:

$$u_{i,L}(x, y, z, t) = F_x^{-1} \{ H_{i,L}(\lambda_x, y) F_x [u_i(x, y_O, z, t)] \}, \quad (1)$$

in which F_x and F_x^{-1} denote the Fourier transform and inverse Fourier transform, respectively, λ_x is the streamwise wavelength, (x, y, z) are the coordinates in streamwise, wall-normal and spanwise directions, respectively, $y_O^+ = 100$ is the outer reference wall-normal height (in inner units) for calculating near-wall footprint (Wang *et al.*, 2021a), and $H_{i,L}$ is the scale-dependent complex-valued kernel function of the spectral lin-

ear stochastic estimation (Baars *et al.*, 2016), which is:

$$H_{i,L}(\lambda_x, y) = \frac{\langle \hat{u}_i(\lambda_x, y, z, t) \overline{\hat{u}_i(\lambda_x, y_O, z, t)} \rangle_{z,t}}{\langle \hat{u}_i(\lambda_x, y_O, z, t) \overline{\hat{u}_i(\lambda_x, y_O, z, t)} \rangle_{z,t}}, \quad (2)$$

where, $\hat{(\cdot)}$ represents variables in Fourier space, $\langle \cdot \rangle_{z,t}$ denotes averaging in spanwise and time.

Causal-analysis methods

Causal discovery or causal inference has recently become one of the most popular topics and a tool to discover the underlying causal structure of physical systems. There is an ever-growing number of methods designed to work under different assumptions since the seminal work of Granger (1969). There are several reviews dedicated to introducing different methods (Pearl, 2009; Liang, 2013; Camps-Valls *et al.*, 2023; Runge *et al.*, 2023). In this study, we choose two widely-used causal-inference methods, *i.e.* transfer entropy and information flow, and apply them to several scenarios including interactions of near-wall inner and outer turbulent motions.

Transfer entropy. The framework of information theory (Shannon, 1948) can be employed to quantify causality among time signals of different variables. A key metric is the transfer entropy (Schreiber, 2000), which has been applied in turbulent-flow problems recently (Lozano-Durán *et al.*, 2020; Wang *et al.*, 2021b, 2022; Martínez-Sánchez *et al.*, 2023).

Here we follow Martínez-Sánchez *et al.* (2023) to calculate the Shannon entropy $S(X)$ of variable X through estimations of the probability density function of each signal using the k -nearest-neighbour entropy estimator (Kozachenko & Leonenko, 1987), as:

$$S(X) = \psi(N) - \psi(k) + \log c_d + \frac{d}{N} \sum_{i=1}^N \log \varepsilon(i), \quad (3)$$

where X is a discrete-valued variable, N is the number of discrete data, $\psi(\cdot)$ donates the digamma function, d is the dimension of X , $c_d = 1$ for the L_∞ -norm, and $\varepsilon(i)$ is the distance from x_i to its k th neighbour.

For a multivariate problem, we use the following formula

$$T_{j \rightarrow i}(\Delta t) = S(V_i(t) | \mathbf{V}^j(t - \Delta t)) - S(V_i(t) | \mathbf{V}(t - \Delta t)), \quad (4)$$

to calculate the conditional transfer entropy (Lizier, 2014; Lozano-Durán *et al.*, 2020), where Δt is the time lag, $S(V_i | \mathbf{V})$ is the conditional Shannon entropy and \mathbf{V}^j is equivalent to \mathbf{V} but excluding the component j . The conditional Shannon entropy is defined by $S(Y|X) = S(X, Y) - S(X)$. Transfer entropy quantifies the amount of uncertainty in a future signal reduced by a past signal. A larger transfer entropy $T_{j \rightarrow i}$ represents a stronger causality from V_j to V_i .

Information flow. Information flow refers to the transfer of information between two entities in a dynamical system. In information-flow theory, the quantity that quantifies causalities is the rate of information flow. Liang & Kleeman (2005) argued that, as a two-dimensional system ($\{x_1, x_2\}$) steers a state forward, the marginal entropy of x_1 is replenished from two different sources: one is from x_1 itself, and

another one from x_2 . The latter is through the very mechanism namely information flow. This gives a decomposition of the marginal entropy increase according to the underlying mechanisms: $dS_1/dt = dS_1^*/dt + L_{2 \rightarrow 1}$, the term dS_1^* is the x_1 own contribution, the other term $L_{2 \rightarrow 1}$ is the rate of information flow from x_2 to x_1 . Liang (2013) firstly established a rigorous formalism of information flow for deterministic and stochastic systems. After that, Liang (2014) used maximum-likelihood estimation to derive an estimation formula for information flow consisting only of correlation. A preliminary application of information flow in turbulence can be found in Liang & Lozano-Durán (2016).

We evaluate multivariate information flow according to Liang (2021), as

$$L_{j \rightarrow i} = \frac{dS_i}{dt} - \frac{dS_{ij}}{dt} \approx \frac{1}{\det(\mathbf{C})} \cdot \sum_{m=1}^d \Delta_{jm} C_{m,di} \cdot \frac{C_{ij}}{C_{ii}}, \quad (5)$$

where C_{ij} is the covariance between V_i and V_j , and $C_{i,dj}$ is the covariance between V_i and \dot{V}_j , \dot{V}_j is the time derivative of V_j , \mathbf{C} is the covariance matrix, $\det(\cdot)$ is the determinant of a matrix, and d is the number of variables. The Δ_{ij} is the cofactors of the covariance matrix. dS_i/dt is the temporal variation rate of $S(V_i)$, and dS_{ij}/dt is the evolution of $S(V_i)$ with the effect of V_j excluded. So, $L_{j \rightarrow i}$ denotes the rate of information flow from V_j to V_i .

In the following, the self-causalities are set to zero. The largest causality is used for normalization so that the causalities are between 0 and 1. The absolute value of the normalized metrics is preserved only if greater than 0.01, otherwise it is set to zero.

RESULTS AND DISCUSSION

Linear problem. First, we study the causalities of a linear problem, which is a six-dimensional vector autoregressive process (Liang, 2021):

$$\begin{aligned} \mathbf{X}(n+1) &= \boldsymbol{\alpha} + \mathbf{A}\mathbf{X}(n) + \mathbf{B}\mathbf{e}(n+1), \\ \mathbf{A} &= \begin{pmatrix} 0 & 0 & -0.6 & 0 & 0 & 0 \\ -0.5 & 0 & 0 & 0 & 0 & 0.8 \\ 0 & 0.7 & 0 & 0 & 0 & 0 \\ 0 & 0 & 0 & 0.7 & 0.4 & 0 \\ 0 & 0 & 0 & 0.2 & 0 & 0.7 \\ 0 & 0 & 0 & 0 & 0 & -0.5 \end{pmatrix}, \\ \boldsymbol{\alpha} &= (0.1, 0.7, 0.5, 0.2, 0.8, 0.3)^T, \end{aligned} \quad (6)$$

where \mathbf{B} is a diagonal matrix with $B_{ii} = 100$ ($i = 1, \dots, 6$), and the errors $e_i \sim N(0, 1)$ are independent variables. We generated 500 independent sets of data consisting of six series with 10000 steps (randomly initialized). The time lag for causal analysis is set to Δt .

The results are shown in figure 1. It shows that the two methods yield the same qualitative causalities in the linear problem, despite some numerical differences. The identified non-zero causalities of $x_1 \rightarrow x_2$, $x_2 \rightarrow x_3$, $x_3 \rightarrow x_1$, $x_4 \rightarrow x_5$, $x_5 \rightarrow x_4$, $x_6 \rightarrow x_2$ and $x_6 \rightarrow x_5$ are consistent with equation (6). Therefore, both the transfer entropy and information flow are effective in evaluating the causalities of the linear problem.

Nonlinear problem. The second case is the causalities of a nonlinear problem. We choose the coupled system

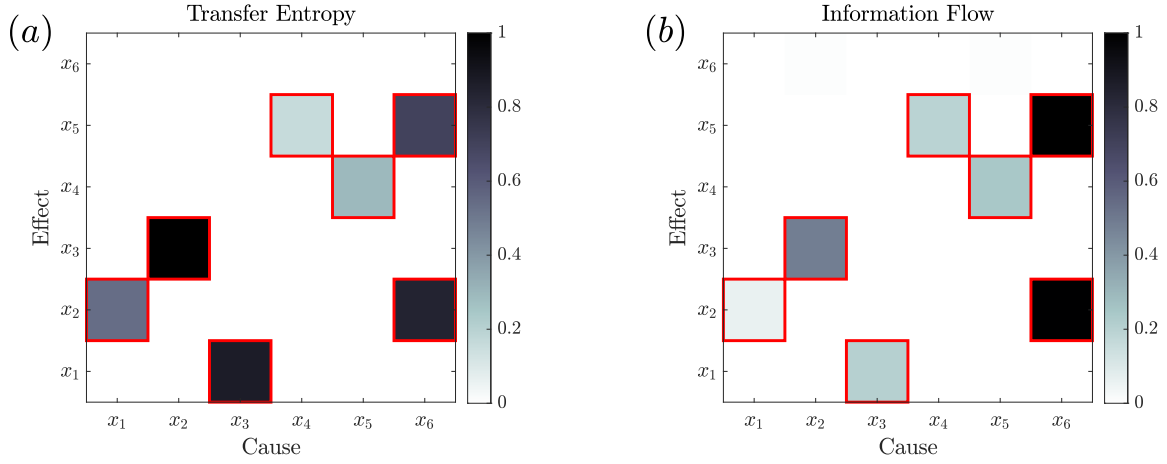


Figure 1. Causal maps of the linear problem: (a) transfer entropy; (b) information flow. Red boxes: causalities identified by both transfer entropy and information flow.

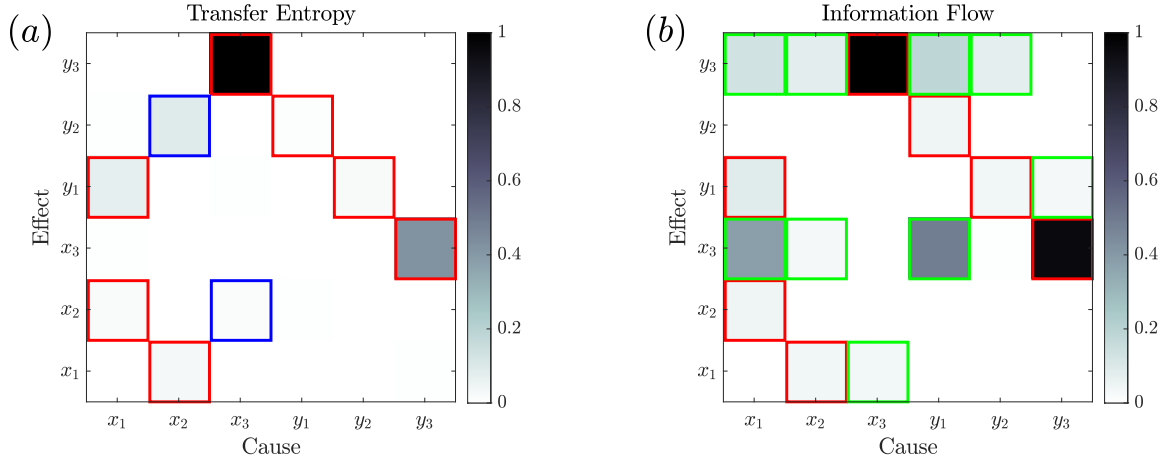


Figure 2. Causal maps of the nonlinear problem: (a) transfer entropy; (b) information flow. Red boxes: causalities identified by both transfer entropy and information flow. Blue boxes: causalities identified by transfer entropy but information flow. Green boxes: causalities identified by information flow but transfer entropy.

investigated by Paluš *et al.* (2018):

$$\begin{cases} dx_1/dt = -\omega_1 x_2(t) - x_3(t), \\ dx_2/dt = \omega_1 x_1(t) + 0.15x_2(t), \\ dx_3/dt = 0.2 + x_3(t) [x_1(t) - 10], \\ dy_1/dt = -\omega_2 y_2(t) - y_3(t) + \varepsilon [x_1(t) - y_1(t)], \\ dy_2/dt = \omega_2 y_1(t) + 0.15y_2(t), \\ dy_3/dt = 0.2 + y_3(t) [y_1(t) - 10], \end{cases} \quad (7)$$

in which $\omega_1 = 1.015$ and $\omega_2 = 0.985$, and ε is set to 0.25. The above nonlinear system is solved using the fourth-order Runge-Kutta scheme with a time step $\Delta t = 0.001$. Initialized with random numbers, the equations are integrated forward for $N = 50000$ steps, in which the first 10000 steps are discarded to eliminate the effects of initial conditions. A total of 500 independent sets of data are generated finally. The time lag for causal analysis is set to $2\Delta t$.

The results are displayed in figure 2. It is seen that the causalities identified by the two metrics are not the same. Both of the two methods can identify the causalities of $x_2 \rightarrow x_1$, $x_1 \rightarrow x_2$, $y_2 \rightarrow y_1$, $x_1 \rightarrow y_1$ and $y_1 \rightarrow y_2$, which exist in equation (7). However, the causalities of $x_3 \rightarrow x_1$, $x_1 \rightarrow x_3$, $y_3 \rightarrow y_1$

and $y_1 \rightarrow y_3$ are missing in the results of transfer entropy, which are preserved in the results of information flow. Therefore, in this nonlinear problem, the information flow is more effective for identifying causalities than the transfer entropy. It is also noted that some identified causalities are not explicitly found in equation (7) which may be attributed to the nonlinear effects.

Low-dimensional model of the near-wall cycle of turbulence.

Next, we analyze the causal relations present in a low-dimensional model of the plane Couette flow with a sinusoidal body force developed by Moehlis *et al.* (2004). This model presents an improvement of the eight-mode model of Waleffe (1997). The self-sustaining process of near-wall turbulence, *i.e.* the streak-vortex cycle, can be well captured by the low-dimensional model. There are nine modes of the model, which are: the basic profile mode (1), the streak mode (2), the downstream vortex mode (3), the spanwise flow modes (4, 5), the normal vortex modes (6, 7), a fully three-dimensional mode (8) and the mode of the modification of the basic profile (9). The first eight modes are the same as those in Waleffe (1997). By applying the Galerkin projection to the Navier-Stokes equations without the pres-

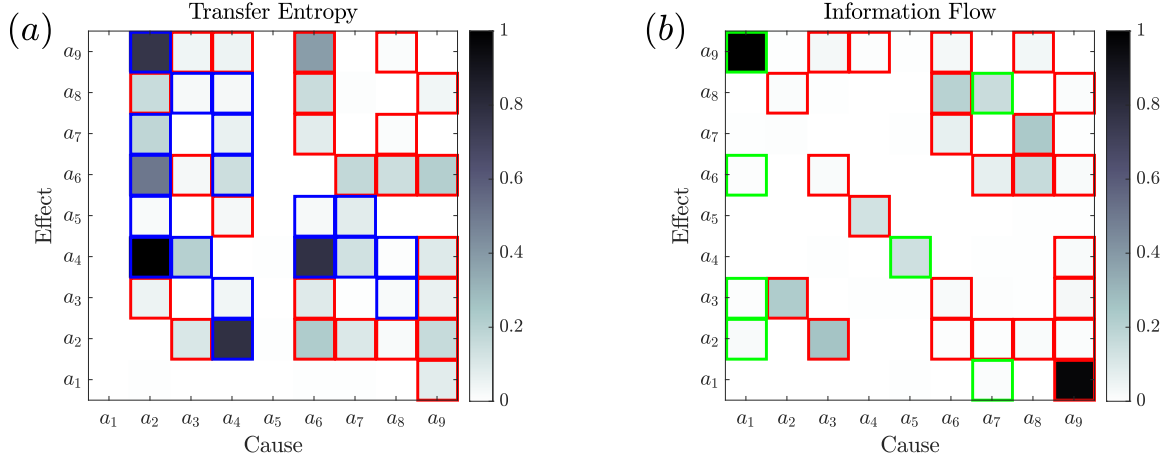


Figure 3. Causal maps of the low-dimensional model of self-sustaining near-wall turbulence: (a) transfer entropy; (b) information flow. **Red boxes:** causalities identified by both transfer entropy and information flow. **Blue boxes:** causalities identified by transfer entropy but information flow. **Green boxes:** causalities identified by information flow but transfer entropy.

sure term, one can obtain a set of nine ordinary differential equations for the temporal amplitude coefficient $a_i(t)$, featuring quadratic nonlinearities. In the present study, we follow Martínez-Sánchez *et al.* (2023) to use the same parameter setup. The ordinary differential equations were numerically solved to obtain 500 sets of solutions, each spanning 4000 time units and the time step is 0.01 time units (400 000 time steps). These data are generated by introducing a random perturbation to a_4 (Martínez-Sánchez *et al.*, 2023). The time lag for the causal analysis is set to one time step.

The results are given in figure 3. It is seen that there are quite a lot of differences between the results of the two approaches. First, we focus on the core sustaining mechanism of near-wall turbulence, *i.e.* the generation of streaks (mode 2). It has been well recognized that the streaks are generated by the streamwise vortex acting on the mean flow, that is the so-called lift-up mechanism. In the low-order model, it is the causality from mode 1 and 3 to mode 2. We can see from figure 3 that the information flow can successfully capture the causal links of $a_1 \rightarrow a_2$ and $a_3 \rightarrow a_2$, while the transfer entropy only can predict $a_3 \rightarrow a_2$. For the other nonlinear interaction mechanism for a_2 , both transfer entropy and information flow can identify the causal links which are present in the dynamical equation of a_2 , except that $a_4 \rightarrow a_2$ is only detected by the transfer entropy. Second, we look into the generation of streamwise vortex (mode 3). Both the transfer entropy and information flow can identify $a_2 \rightarrow a_3$ (streak to streamwise vortex), $a_6 \rightarrow a_3$ (normal vortex to streamwise vortex), and $a_9 \rightarrow a_3$. However, the causal links of $a_4 \rightarrow a_3$ (spanwise flow to streamwise vortex) and $a_8 \rightarrow a_3$ (three-dimensional mode to streamwise vortex), which exist in the dynamical equation of a_3 , can be found in the result of the transfer entropy analysis, but that of the information flow. Lastly, if further surveying other modes, one can find that the transfer entropy can identify more causal links in the dynamical equations than the information flow.

Near-wall inner and outer turbulent motions. Finally, we apply the transfer entropy and information flow to analyze the causalities of inner and outer motions of near-wall turbulence. A time-resolved direct numerical simulation (DNS) of turbulent channel flow at a friction Reynolds number of $Re_\tau = 1000$ is carried out in this work. The DNS

adopts a fourth-order accurate compact difference scheme in the homogeneous directions and a second-order accurate central difference scheme in the wall-normal direction for the discretization of the incompressible Navier-Stokes equations on a staggered grid (Hu *et al.*, 2018). A series of low-Reynolds-number channel DNS (up to $Re_\tau = 600$) were conducted using the code (Hu & Zheng, 2018; Wang *et al.*, 2021a) and the results were well validated against Lee & Moser (2015). In the present DNS, the flow time span is $19.8\delta/u_\tau$ (δ is channel half-height and u_τ is the friction velocity) and the DNS data are stored with a time step of $\Delta t = 0.03$ (20 000 snapshots in total). The transfer entropy in equation (4) is estimated using a time lag $\Delta t = 0.03$ and the nearest-neighbour parameter $k = 4$ following Martínez-Sánchez *et al.* (2023).

Figure 4 shows the causal maps of local velocity fluctuations of inner and outer turbulent motions and pressure fluctuations, *i.e.* $\mathbf{V} = (u_S, v_S, w_S, u_L, v_L, w_L, p)$, where u , v and w are the streamwise, wall-normal and spanwise velocity fluctuations, respectively, and p is pressure fluctuation. The subscripts "S" and "L" indicate inner and outer motions, respectively. The time series of local velocity and pressure fluctuations at 10 000 random locations at $y^+ = 15$ are adopted to calculate the causalities. It is seen that there are many more causalities identified by the transfer entropy including all of those by the information flow. On the other hand, the compactness of the causal links identified by the information flow could provide a concise picture that helps to find the most crucial causalities. For example, one can find the causal links of $u_S \leftrightarrow v_S$ and $u_L \leftrightarrow v_L$, which are the streak-vortex self-sustaining cycles of inner and outer motions, respectively. It is also seen that there exists a non-zero causality of $u_S \rightarrow v_L$, indicating a possible bottom-up generation mechanism for the wall-normal outer motions. The pressure fluctuation is also found to be an active component in the causal cycles with inner and outer motions.

Figure 5 shows the causal maps of the local velocity and pressure fluctuations of inner and outer turbulent motions at $y^+ = 70$. Compared to figure 4, more causal links can be identified as the outer motions are stronger. Similar to figure 4, the transfer entropy can predict more causalities than the information flow. However, we still discuss the results focusing on the causal links that can be identified by both the transfer entropy and information flow. Similarly, the inner and outer self-sustaining causalities of the streak-vortex cycle can also

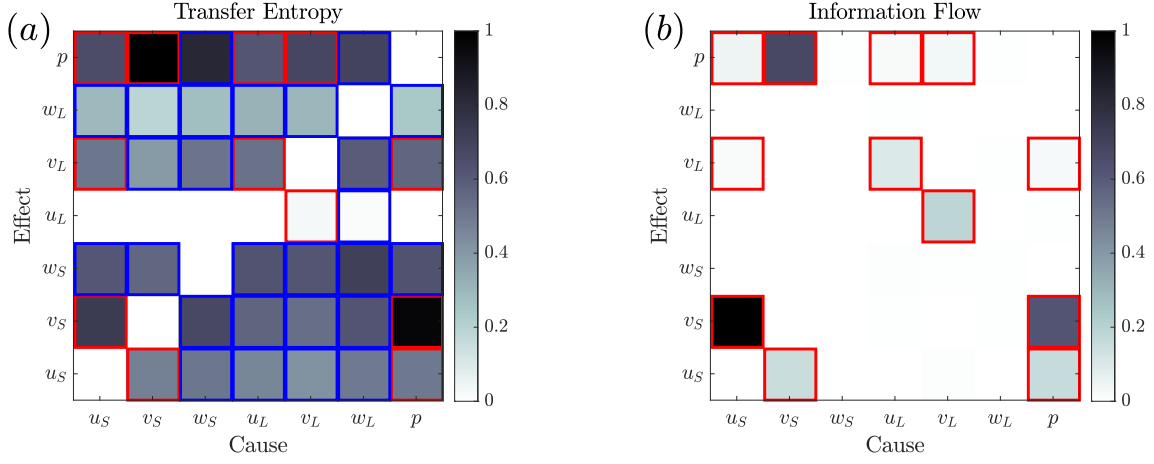


Figure 4. Causal maps of the inner and outer motions of near-wall turbulence at $y^+ = 15$: (a) transfer entropy; (b) information flow. **Red boxes**: causalities identified by both transfer entropy and information flow. **Blue boxes**: causalities identified by transfer entropy but information flow. **Green boxes**: causalities identified by information flow but transfer entropy.

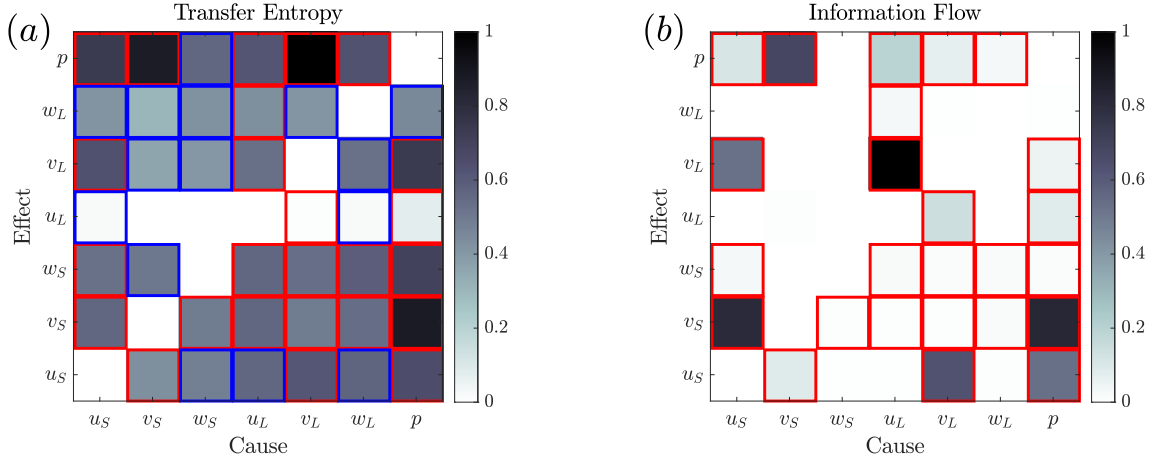


Figure 5. Causal maps of inner and outer motions of near-wall turbulence at $y^+ = 70$: (a) transfer entropy; (b) information flow. **Red boxes**: causalities identified by both transfer entropy and information flow. **Blue boxes**: causalities identified by transfer entropy but information flow. **Green boxes**: causalities identified by information flow but transfer entropy.

be well observed at this height as well as the bottom-up causality of $u_S \rightarrow v_L$ and the pressure-velocity causalities. In addition, two new groups of links with non-zero causalities can be found. The first one includes $u_S \rightarrow w_S$, $u_L \rightarrow w_L$ and $w_S \rightarrow v_S$, which may be related to the streak instabilities and generation of streamwise vortex. The other one reflects the top-down influence, like $(u_L, v_L, w_L) \rightarrow (u_S, v_S, w_S)$. These results indicate that the inner and outer turbulent motions are not only self-sustained but also engage in complex interaction mechanisms that we may not fully understand at the current stage.

SUMMARY

In this work, we have applied two popular causal-analysis methods, *i.e.* transfer entropy and information flow, to several problems from simple linear and nonlinear dynamical systems to complex turbulent flows. The two methods can predict the same results for the linear problem, but some differences exist for the other nonlinear problems and the complex turbulent-flow problems. To be more specific, more causal links that exist in the dynamical system can be revealed by the information flow in the nonlinear problem. However, for the low-dimensional model of the near-wall cycle of turbulence,

it seems that richer causalities can be identified by the transfer entropy. Despite this, both methods can capture the major self-sustaining mechanism of near-wall turbulence, *i.e.* the streak-vortex regeneration cycle. Some insight into the inner and outer near-wall turbulent motions has been achieved through the present causal analysis. The inner and outer motions may be not only self-sustained but also exhibit non-negligible influence on each other, beyond the common opinion of either bottom-up or top-down, and more details on these will be investigated in future work.

Lastly, we need to mention that the computation is time-consuming using the transfer entropy for high-dimensional problems, while it is much more efficient with the information flow (nearly a hundred of speed-up in our experience). Therefore, we believe that the information flow may have great potential in applications of causal inference for turbulent-flow problems besides the transfer entropy.

ACKNOWLEDGEMENT

The authors are grateful to Prof. X. San Liang for very helpful discussions.

REFERENCES

- Adrian, RJ 2007 Hairpin vortex organization in wall turbulence. *Physics of Fluids* **19** (4), 041301.
- Adrian, RJ, Meinhart, CD & Tomkins, CD 2000 Vortex organization in the outer region of the turbulent boundary layer. *Journal of Fluid Mechanics* **422**, 1–54.
- Baars, WJ, Hutchins, N & Marusic, I 2016 Spectral stochastic estimation of high-Reynolds-number wall-bounded turbulence for a refined inner-outer interaction model. *Physical Review Fluids* **1** (5), 054406.
- Camps-Valls, G *et al.* 2023 Discovering causal relations and equations from data. *Physics Reports* **1044**, 1–68.
- Cossu, C & Hwang, Y 2017 Self-sustaining processes at all scales in wall-bounded turbulent shear flows. *Philosophical Transactions of the Royal Society A: Mathematical, Physical and Engineering Sciences* **375** (2089).
- Granger, CWJ 1969 Investigating causal relations by econometric models and cross-spectral methods. *Econometrica* **37** (3), 424–438.
- Hamilton, JM, Kim, J & Waleffe, F 1995 Regeneration mechanisms of near-wall turbulence structures. *Journal of Fluid Mechanics* **287**, 317–348.
- Hu, R, Wang, L, Wang, P, Wang, Y & Zheng, X 2018 Application of high-order compact difference scheme in the computation of incompressible wall-bounded turbulent flows. *Computation* **6** (2), 31.
- Hu, R & Zheng, X 2018 Energy contributions by inner and outer motions in turbulent channel flows. *Physical Review Fluids* **3** (8), 084607.
- Hunt, JCR & Morrison, JF 2000 Eddy structure in turbulent boundary layers. *European Journal of Mechanics - B/Fluids* **19** (5), 673–694.
- Hutchins, N & Marusic, I 2007 Evidence of very long meandering features in the logarithmic region of turbulent boundary layers. *Journal of Fluid Mechanics* **579**, 1–28.
- Jiménez, J 2018 Coherent structures in wall-bounded turbulence. *Journal of Fluid Mechanics* **842**, P1.
- Kozachenko, LF & Leonenko, NN 1987 Sample estimate of the entropy of a random vector. *Problemy Peredachi Informatsii* **23** (2), 9–16.
- Lee, MK & Moser, RD 2015 Direct numerical simulation of turbulent channel flow up to $Re_\tau \approx 5200$. *Journal of Fluid Mechanics* **774**, 395–415.
- Liang, XS 2013 The Liang-Kleeman information flow: Theory and applications. *Entropy* **15** (1), 327–360.
- Liang, XS 2014 Unraveling the cause-effect relation between time series. *Physical Review E* **90** (5), 052150.
- Liang, XS 2016 Information flow and causality as rigorous notions *ab initio*. *Physical Review E* **94** (5), 052201.
- Liang, XS 2021 Normalized multivariate time series causality analysis and causal graph reconstruction. *Entropy* **23** (6), 679.
- Liang, XS & Kleeman, R 2005 Information transfer between dynamical system components. *Physical Review Letters* **95** (24), 244101.
- Liang, XS & Lozano-Durán, A 2016 A preliminary study of the causal structure in fully developed near-wall turbulence. *CTR Proc. of the Summer Prog* p. 233.
- Lizier, JT 2014 JIDT: An information-theoretic toolkit for studying the dynamics of complex systems. *Frontiers in Robotics and AI* **1**, 11.
- Lozano-Durán, A, Bae, HJ & Encinar, MP 2020 Causality of energy-containing eddies in wall turbulence. *Journal of Fluid Mechanics* **882**, A2.
- Martínez-Sánchez, Á, López, E, Le Clainche, S, Lozano-Durán, A, Srivastava, A & Vinuesa, R 2023 Causality analysis of large-scale structures in the flow around a wall-mounted square cylinder. *Journal of Fluid Mechanics* **967**, A1.
- Marusic, I, Mathis, R & Hutchins, N 2010 Predictive model for wall-bounded turbulent flow. *Science* **329** (5988), 193–196.
- Mathis, R, Hutchins, N & Marusic, I 2011 A predictive inner-outer model for streamwise turbulence statistics in wall-bounded flows. *Journal Fluid Mechanics* **681**, 537–566.
- Moehlis, J, Faisst, H & Eckhardt, B 2004 A low-dimensional model for turbulent shear flows. *New Journal of Physics* **6** (1), 56.
- Paluš, M, Krakovská, A, Jakubík, J & Chvosteková, M 2018 Causality, dynamical systems and the arrow of time. *Chaos: An Interdisciplinary Journal of Nonlinear Science* **28** (7).
- Pearl, J 2009 Causal inference in statistics: An overview. *Statistics Surveys* **3**, 96–146.
- Robinson, SK 1991 Coherent motions in the turbulent boundary layer. *Annual Review of Fluid Mechanics* **23**, 601–639.
- Runge, J *et al.* 2023 Causal inference for time series. *Nature Reviews Earth & Environment* **4** (7), 487–505.
- Schreiber, T 2000 Measuring information transfer. *Physical Review Letters* **85** (2), 461.
- Shannon, CE 1948 A mathematical theory of communication. *The Bell System Technical Journal* **27** (3), 379–423.
- Smits, AJ, McKeon, BJ & Marusic, I 2011 High-Reynolds number wall turbulence. *Annual Review of Fluid Mechanics* **43**, 353–375.
- Toh, S & Itano, T 2005 Interaction between a large-scale structure and near-wall structures in channel flow. *Journal of Fluid Mechanics* **524** (2005), 249–262.
- Waleffe, F 1997 On a self-sustaining process in shear flows. *Physics of Fluids* **9** (4), 883–900.
- Wang, L, Hu, R & Zheng, X 2021a A scaling improved inner-outer decomposition of near-wall turbulent motions. *Physics of Fluids* **33** (4), 045120.
- Wang, W, Lozano-Durán, A, Helmig, R & Xu, C 2022 Spatial and spectral characteristics of information flux between turbulent boundary layers and porous media. *Journal of Fluid Mechanics* **949**, A16.
- Wang, W, Xu, C, Lozano-Durán, A, Helmig, R & Weigand, B 2021b Information transfer between turbulent boundary layers and porous media. *Journal of Fluid Mechanics* **920**, A21.
- Zhou, Z, Xu, C-X & Jiménez, J 2022 Interaction between near-wall streaks and large-scale motions in turbulent channel flows. *Journal of Fluid Mechanics* **940**, A23.